Available online at www.sciencedirect.com

ScienceDirect

Scripta Materialia 84–85 (2014) 27–30

Scripta MATERIALIA

www.elsevier.com/locate/scriptamat

Ultrahigh-strength submicron-sized metallic glass wires

Y.B. Wang,[a] C.C. Lee,[a,b] J. Yi,[c] X.H. An,[a] M.X. Pan,[c] K.Y. Xie,[a,b] X.Z. Liao,[a,*] J.M. Cairney,[a,b] S.P. Ringer[a,b] and W.H. Wang[c,*]

[a]*School of Aerospace, Mechanical and Mechatronic Engineering, The University of Sydney, Sydney, NSW 2006, Australia*
[b]*Australian Centre for Microscopy and Microanalysis, The University of Sydney, Sydney, NSW 2006, Australia*
[c]*Institute of Physics, Chinese Academy of Sciences, Beijing 100080, People's Republic of China*

Received 1 April 2014; revised 11 April 2014; accepted 11 April 2014
Available online 18 April 2014

In situ deformation experiments were performed in a transmission electron microscope to investigate the mechanical properties of submicron-sized $Pd_{40}Cu_{30}Ni_{10}P_{20}$ metallic glass (MG) wires. Results show that the submicron-sized MG wires exhibit intrinsic ultrahigh tensile strength of ~2.8 GPa, which is nearly twice as high as that in their bulk counterpart, and ~5% elastic strain approaching the elastic limits. The tensile strength, engineering strain at failure and deformation mode of the submicron-sized MG wires depend on the diameter of the wires.

Keywords: Metallica glass; Mechanical property; Size effects; Transmission electron microscopy

Metallic glasses (MGs) show good potential for applications as micro- and nanoelectromechanical devices because they possess excellent mechanical properties [1–5]. The utilization of MGs in micro- or nanotechnological systems requires a thorough understanding of their mechanical behaviour; in particular, strength and ductility are key issues. It was recently reported that the deformation mechanisms, and consequently the mechanical behaviour of crystalline materials, depend significantly on the sample size when the sample dimensions are in the micrometre and nanometre ranges [6–8]. Specifically, the tensile strength of single crystal metallic pillars has been shown to increase significantly with decreasing pillar diameter, which is attributed to dislocation starvation in small volumes [7,8]. However, this strengthening mechanism is not thought to operate in MGs due to their glassy atomic structure and the absence of lattice dislocations. Nevertheless, numerous investigations have demonstrated similar size effects on the deformation behaviour of MG pillar samples fabricated using the focused ion beam (FIB) technique [9–13]. For example, while the strength of MGs in the bulk form is controlled by shear band propagation, the strength of MGs with dimensions in the micrometre/sub-micrometre regime and in the nanometre range is determined by shear band nucleation and uniform shear transformation zones, respectively [11]. Further, when the dimensions of MG samples are smaller than 100 nm, a brittle-to-ductile transition occurs without compromising the strength of the material [14,15].

One-dimensional crystalline nanowires (NWs) have been widely and successfully used in nanodevices [16,17]. The mechanical properties of these crystalline NWs are significantly influenced by defects [18]. Theoretical predictions and experimental observations demonstrate that the surface structures of metallic and semiconducting NWs severely affect their elastic moduli [19,20]. In contrast, MGs do not possess any structural defects such as dislocations or grain boundaries, and this is widely thought to explain why they usually exhibit such good mechanical properties [1–4]. This, coupled with the stability of these properties, has stimulated much interest in exploring MGs as candidate materials for applications in nanoelectromechanical systems [21].

FIB milling has been the most successful technique used to date to fabricate nanoscale MG samples in order to investigate their mechanical properties. The Ga ion bombardment that takes place during the FIB sample preparation inevitably induces irradiation damage to

* Corresponding authors; e-mail addresses: xiaozhou.liao@sydney.edu.au; whw@iphy.ac.cn

http://dx.doi.org/10.1016/j.scriptamat.2014.04.005
1359-6462/

the surface layer of the material, which significantly alters its mechanical behaviour [22,23], thereby making it difficult to determine the intrinsic mechanical properties at the nanoscale. Few alternative fabrication techniques that do not involve FIB have been used to produce nano- and submicron-sized MG samples, and very little is known about the mechanical properties of submicron-sized MG wires produced using such alternative fabrication techniques. This is an unsatisfactory state of knowledge because it suggests that we are yet to measure the true, intrinsic mechanical properties of these materials. In this work, we produced submicron-sized MG wires without FIB, and explored the mechanical properties of the submicron-sized MG wires using in situ tensile testing in a transmission electron microscope (TEM). We discovered that the ultimate tensile strength and engineering strain of MG wires depend heavily on their diameter. Reducing the diameter of such wires to ~340 nm almost doubles their tensile strength compared to that of bulk MG, with values as high as 2.8 GPa being recorded. Moreover, the reduced diameter of the wires leads to a dramatic increase in elastic strain, from ~2% in the bulk to ~5%.

Figure 1a shows typical $Pd_{40}Cu_{30}Ni_{10}P_{20}$ (at.%) MG wires with lengths of more than 200 μm. The wires appear as white lines on a dark silicon support. An enlarged image of the position indicated with an arrow in Figure 1a is presented in Figure 1b, revealing that the MG wires produced in this way have a homogeneous smooth surface structure. These microscopic images indicate that the structural quality of these submicron-sized MG wires is higher than that of the Zr-based MG NWs produced at the fracture surface of a bulk MG through a conventional mechanical testing process [24]. The very high structural quality of these MG wires further supports our objective to obtain reliable intrinsic mechanical property data from the MGs whilst avoiding the various testing-type artefacts arising from structural inhomogeneities and the FIB-induced surface defects that have occurred in previous MG NW studies [22,23,25,26].

Figure 2a is a scanning electron microscope (SEM) image of an MG wire of diameter ~1230 nm bridging the gap of a push-to-pull (PTP) module. The two ends of the wire were welded onto the module using Pt under an FIB. An enlarged view of the welded joint is provided in the inset SEM image, which clearly shows that the joint is sound and defect free. Figure 2b, which was extracted from Movie 1 in the Supporting information, shows that the fracture of the wire caused by in situ tensile deformation occurred via several shear banding

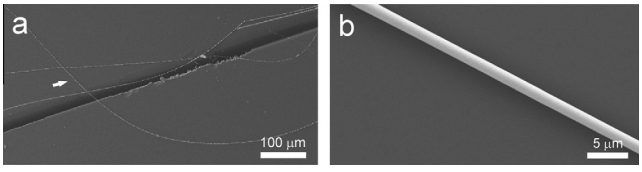

Fig. 1. (a) A SEM image of $Pd_{40}Cu_{30}Ni_{10}P_{20}$ metallic glass wires. (b) An enlarged image of the wire indicated by the white arrow in (a), revealing a high-quality wire with a homogeneous smooth surface structure, with no defects.

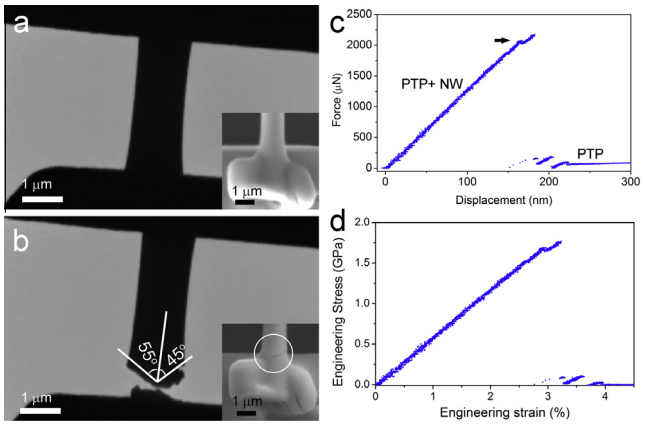

Fig. 2. (a) A TEM bright-field image showing a $Pd_{40}Cu_{30}Ni_{10}P_{20}$ MG wire bridging the gap of a PTP module. The inset SEM image shows one end of the wire before tensile straining. (b) A TEM image extracted from Movie 1 showing a brittle fracture caused by in situ straining. The inset SEM image shows the fracture after deformation. (c) The force–displacement curve from the combined contribution of the PTP module and the wire. The kink indicated by the black arrow suggests a crack initiation followed by fracture. (d) The engineering stress–strain curve for the wire after subtracting the contribution from the PTP module.

events. The fracture angles relative to the wire axial direction (indicated by white lines in Fig. 2b) are about 55° and 45° at each side of the wire, which is a typical brittle fracture feature in BMG samples, as previously reported [27]. After retracting the applied external force, the two fractured ends of the wire are in contact owing to the reversible elastic deformation of the PTP module. However, the fracture is still visible, as shown in the circled position in the inset SEM image. Figure 2c presents the corresponding force–displacement curve, which combines the contributions from the PTP module and the wire. The force increased linearly up to ~2035 μN (as indicated by a black arrow), when kinking occurred. The kink corresponds to a crack initiation on the left side of the wire that approached the lower welding point, as shown in Movie 1. After the kink, the force continued to increase linearly until the wire fractured at ~2150 μN. Further pushing of the PTP led to an immediate drop in force down to ~150 μN, coupled with some force vibration induced by the detachment between the two parts of the wire, then a further drop to ~60 μN. After that, the force increased linearly again because of the stiffness of the empty PTP. The engineering stress–strain curve of the wire shown in Figure 2d was obtained by removing the contribution of the PTP module from Figure 2c and then converting the net force applied to the wire and the displacement into stress and strain, respectively. The tensile strength of ~1.75 GPa shown in Figure 2d is slightly higher than the 1.6–1.7 GPa reported for bulk Pd-based MGs [28,29]. There was no notable plastic strain in the wire.

The mechanical behaviour of MG wires varies with their diameters. Figure 3 shows a typical mechanical behaviour of a submicron-sized MG wire with a diameter of 340 nm. The in situ tensile straining process was recorded in Movie 2 in the Supporting information and the wire images before deformation and after frac-

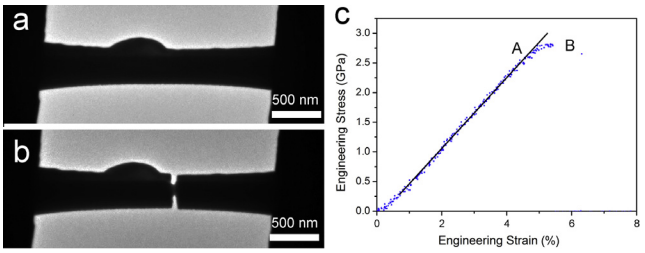

Fig. 3. (a) A TEM bright-field image of an MG wire with a diameter of 340 nm. (b) A TEM image extracted from Movie 2 showing necking during in situ straining. (c) The engineering stress–strain curve for the wire; points A and B indicate the yielding strength and ultimate tensile strength, respectively.

ture are shown in Figure 3a and b, respectively. Our experiment shows that necking appeared in the submicron-sized wire during tensile deformation, suggesting plastic deformation similar to that in ductile metallic materials. This is in contrast with the highly localized catastrophic fracture via shear banding in the wires with large diameters (see Fig. 2b). A previous report suggests that non-freestanding MG samples can prevent/delay continuous shearing, inducing necking and plasticity [15]. In our research, the wires are freestanding, which is completely different from the situation reported in Ref. [15]. The engineering stress–strain curve in Figure 3c shows that the tensile stress increased linearly before yielding at ~2.68 GPa (point A) and that slight work hardening occurred during the plastic deformation. Failure occurred at the maximum stress of ~2.8 GPa (point B). Based on the evidence presented here, the plastic tensile strain of ~1% (between points A and B) occurred via necking. Note that the tensile ductility for Pd-based MGs [28] in the bulk form and in wires with large diameters (Fig. 2) is near zero. Although necking in MG samples fabricated by FIB [14,15] during tensile experiments has been reported previously, the ductility was likely induced by the FIB processes [22,23]. Our experiments reveal the intrinsic mechanical properties of submicron-sized MG wires because no FIB technique was used for sample preparation.

Figure 4 shows how diameter affects the tensile engineering strain and stress of MG wires at failure. Decreasing the wire diameter from 1230 to 340 nm leads to an increase in engineering elastic strain from ~3.2 to 5% (note that the ideal elastic strain limit of MGs has been reported to be ~5% [30]) and in engineering stress from 1.75 to 2.8 GPa. The tensile strength observed in

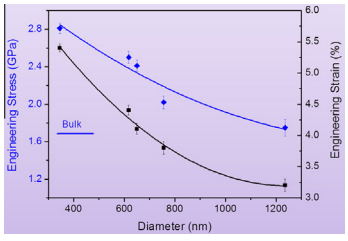

Fig. 4. Relationships between engineering stress, engineering strain and diameter of MG wires obtained from in situ TEM tensile experiments.

the submicron-sized wire with a diameter of 340 nm is ~60% larger than that of the wire with a diameter of 1230 nm and nearly doubles that of its bulk counterpart [28]. MG wires with different diameters were produced from the same precursor with a uniform composition and subjected to the same cooling rate without annealing. Therefore, the only structural variable (other than composition, cooling rate and annealing discussed by Kumar et al. [31]) that leads to different mechanical behaviour of the MG wires is the diameter of the wires. The size effect on the strength of MGs has been controversial. While some investigations have presented evidence showing that smaller is stronger [9–11,14,32,33], other reports demonstrate no size effect on yield strength [34]. This discrepancy may result from the pillar's tapering angle induced by the FIB fabrication technique and Ga ion injection during sample preparation [22,23,33,35]. Our experimental results were obtained from samples that were not affected by any FIB-induced defect and therefore the results are expected to be true.

A significant size effect also applies to the deformation mode, i.e. the deformation mode transfers from localized shear banding to more homogeneous deformation with reduction of the diameter of the MG wires. The critical dimension for the transition of the deformation mode should be between 340 nm, where homogeneous deformation occurs, and 600 nm, where failure by shear banding is still observed. It is expected that homogeneous tensile deformation with larger plastic strain will occur in nanosized wires with diameters smaller than 340 nm.

To understand the reason for the size effect on the strength of MGs, it is useful to consider the stress needed for shear band propagation. The stress σ needed to activate the propagation of a shear band in a submicron-sized MG wire with a diameter of d can be estimated by analogy with crack propagation and can be expressed as [14,36]

$$\sigma = \sqrt{2^{3/2}\Gamma E/ad}$$

where Γ is the the energy per unit area of the shear band and can be estimated by using the measured flow stress and a typical shear band thickness of 10 nm [37], E is the Young's modulus and a is the length-to-diameter ratio. From the formula, the critical stress needed to propagate a shear band is inversely proportional to the square root of the diameter, i.e. the critical stress increases with reducing the diameter. The σ–d curve intersects the stress required to initiate room temperature homogeneous flow at a certain diameter d. The stress for room-temperature homogeneous flow is independent of size and has a value range that is bounded by the ideal strength (upper limit) and the room-temperature elastic limit (lower limit) [14]. The intersection of these two curves is defined as the critical diameter d^*. When the wire diameter d is larger than the critical d^*, the stress needed for shear band propagation is lower than that for homogeneous deformation and the MGs will experience catastrophic failure through shear band propagation (Fig. 2b), as reported in bulk MGs [28]. When the sample size is smaller than d^*, the deformation proceeds

in a homogeneous way. d^* was reported to be ~400 nm in a $Pd_{77}Si_{23}$ MG [36], which is in agreement with the results presented in this study.

The transformation of the deformation mode at the critical d^* value can be further understood from the following aspects: (i) the dimension and number of extrinsic flaws in MG structure that would act as stress concentration sites reduce significantly with decreasing wire diameter, which reduces the probability of the initiation of severely localized plastic deformation via shear banding. Without any runaway shear banding event, individual shear-transformation zones and locally redistributed free volume have the opportunity to mediate multiple atomic-level shear events throughout the samples; (ii) for wires with diameters smaller than d^*, the stress needed for shear band propagation is much larger than that for homogeneous deformation, which has been reported in MG samples fabricated using FIB [14,33]. This can also be explained by the fact that the elastic strain stored in a deformed sample is proportional to its volume, i.e. it scales with d^3 (d is the sample dimension), whereas the surface energy a crack has to overcome scales with d^2. When the diameter decreases, d^3 reduces much faster than d^2, so brittle fracture is more difficult in a small volume. As a result, necking appears (Fig. 3); and (iii) a length scale of the order of 50–500 nm is necessary for a shear band embryo to evolve into a fully developed shear band because the shear band requires a running distance to accelerate to its full propagation speed [5]. Wires below the critical diameter might not be able to provide such a distance and therefore single runaway failure is difficult. Meanwhile, local atomic-level flow events are able to participate in the accommodation of the imposed strain, contributing to deformation. Therefore, a neck may develop before fracture.

In summary, submicron-sized $Pd_{40}Cu_{30}Ni_{10}P_{20}$ MG wires exhibit an intrinsic ultrahigh tensile strength of ~2.8 GPa, which is nearly twice as high as that in their bulk counterpart, and an elastic strain of ~5%. The tensile strength, engineering strain at failure and deformation mode of the submicron-sized MG wires depend on the diameter of the wires. The fabrication of submicron-sized MG wires with outstanding mechanical properties is attractive for many applications in microelectromechanical systems.

The authors are grateful for the scientific and technical input and support from the Australian Microscopy and Microanalysis Research Facility node at the University of Sydney: Sydney Microscopy & Microanalysis. The authors also acknowledge the financial support from the Australian Research Council and the NSF of China (Grant No. 51171204).

Supplementary data associated with this article can be found, in the online version, at http://dx.doi.org/10.1016/j.scriptamat.2014.04.005.

[1] A.L. Greer, E. Ma, MRS Bull. 32 (2007) 611.
[2] A. Inoue, Acta Mater. 48 (2000) 279.
[3] A. Peker, W.L. Johnson, Appl. Phys. Lett. 63 (1993) 2342.
[4] M.F. Ashby, A.L. Greer, Scripta Mater. 54 (2006) 321.
[5] C.A. Schuh, T.C. Hufnagel, U. Ramamurty, Acta Mater. 55 (2007) 4067.
[6] Z.W. Shan et al., Nat. Mater. 7 (2008) 115.
[7] M.D. Uchic, D.M. Dimiduk, J.N. Florando, W.D. Nix, Science 305 (2004) 986.
[8] J.R. Greer, W.C. Oliver, W.D. Nix, Acta Mater. 53 (2005) 1821.
[9] O.V. Kuzmin, Y.T. Pei, J.T.M. De Hosson, Scripta Mater. 67 (2012) 344.
[10] Y.B. Wang et al., Acta Mater. 60 (2012) 253.
[11] C.C. Wang et al., Acta Mater. 60 (2012) 5370.
[12] C.Q. Chen et al., Phys. Rev. B 83 (2011) 180201.
[13] O.V. Kuzmin, Y.P. Pei, J.T.M. De Hosson, Appl. Phys. Lett. 98 (2011) 233104.
[14] D.C. Jang, J.R. Greer, Nat. Mater. 9 (2010) 215.
[15] H. Guo et al., Nat. Mater. 6 (2007) 735.
[16] S.J. Tans, A.R.M. Verschueren, C. Ekker, Nature 393 (1998) 49.
[17] Y. Xia et al., Adv. Mater. 15 (2003) 353.
[18] B. Peng et al., Nat. Nanotechnol. 3 (2008) 326.
[19] M.T. McDowell, A.M. Leach, K. Gall, Nano Lett. 8 (2008) 3613.
[20] Y.B. Wang et al., Adv. Mater. 23 (2011) 1356.
[21] G. Kumar, H.X. Tang, J. Schroers, Nature 457 (2009) 868.
[22] S.W. Lee, D. Mordehai, E. Rabkin, W.D. Nix, J. Mater. Res. 26 (2011) 1653.
[23] D.J. Magagnosc et al., Sci. Rep. 3 (2013) 1096.
[24] K.S. Nakayama et al., Nano Lett. 8 (2008) 516.
[25] J. Das et al., Phys. Rev. Lett. 94 (2005) 205501.
[26] Y.B. Wang et al., Scripta Mater. 55 (2006) 469.
[27] Z.F. Zhang, J. Eckert, L. Schultz, Acta Mater. 51 (2003) 1167.
[28] T. Mukai, T.G. Nieh, Y. Kawamura, A. Inoue, K. Higashi, Scripta Mater. 46 (2002) 43.
[29] K.F. Yao, F. Ruan, Y.Q. Yang, N. Chen, Appl. Phys. Lett. 88 (2006) 122106.
[30] L. Tian et al., Nat. Commun. 3 (2012) 609.
[31] G. Kumar, P. Neibecker, Y.H. Liu, J. Schroers, Nat. Commun. 4 (2013) 1536.
[32] O.V. Kuzmin, Y.T. Pei, C.Q. Chen, J.T.M. De Hosson, Acta Mater. 60 (2012) 889.
[33] A. Bharathula, S.W. Lee, W.J. Wright, K.M. Flores, Acta Mater. 58 (2010) 5789.
[34] C.Q. Chen, Y.T. Pei, J.T.M. De Hosson, Acta Mater. 58 (2010) 189.
[35] B.E. Schuster, Q. Wei, T.C. Hufnagel, K.T. Ramesh, Acta Mater. 56 (2008) 5091.
[36] C.A. Colkert, A. Donohue, F. Spaepen, J. Appl. Phys. 103 (2008) 083539.
[37] W.L. Johnson, Mater. Res. Soc. Bull. 24 (1999) 42.